Parameter Identification of Free-Floating Robots with Flexible Appendages and Fuel Sloshing

Wolfgang Rackl and Roberto Lampariello

***Abstract*— In this paper we adressed the effects of flexibilities and liquid fuel sloshing on the on-orbit robotics-based dynamic parameter identification. For modelling the liquid fuel sloshing we combined the general free-floating robot dynamics with a mechanical pendulum equivalent model. For the dynamic parameter identification we extended our identification algorithm for rigid body systems to account for these two effects. The flexible and sloshing modes are excited only with the manipulator executing optimized trajectories. For the identification algorithm we make use of the robotic joint position and torque sensor data as well as of on board GNC sensor data. Numerical simulations showed that the two effects can have significant influence to the free-floating dynamics. Furthermore, we showed that the extended parameter identification algorithm improves the accuracy of the dynamic model.**

I. INTRODUCTION

A. Motivation

Future on-orbit servicing (OOS) applications for free-flying robots will involve complex tasks which require high system performance like reliability, efficiency and safety, either in full or shared autonomy or in tele-operation.

The majority of both servicer systems and client satellites are equipped with flexible appendages like solar panels, antennas or certain flexible instruments. Furthermore OOS systems will have fuel tanks on board in order to control attitude and orbit. During an OOS mission the servicer system will make among other tasks fly arounds, far and close approach maneuvers, grasping the target (a so-called client), stabilize, repairing tasks and deorbit the whole system. These tasks will consume fuel and will excite flexible and fuel sloshing modes either on the servicer and/or the client. The OOS system must be able to cope with these conditions to ensure the required safety and high performance. To improve path planning and tracking capabilities as well as efficiency in energy consumption by reducing the control effort, the dynamic model must be known to a sufficient accuracy.

Normally, the manipulator properties stay constant in space, but due to fuel consumption the parameters of the satellite base will change significantly. Especially the fill level has a clear effect to the ratio of fixed fuel mass and slosh fuel mass. The smaller the fill level, the higher the influence of the sloshing mass compared to the fixed fuel mass (see [1]). For an OOS mission this means an increasing sloshing effect towards the end of the mission.

For this reasons, a parameter identification method is indispensable to obtain the inertial parameters like mass, center of mass and moments of inertia of all system components, especially the satellite base and the unknown target.

In this paper, we focus on flexibilities and fuel sloshing effects in the free-floating dynamics and the related parameter identification. The Reduced Dynamics Algorithm (RDA) method to identify the parameter of a rigid body system we proposed in [2] was extended separately to both effects. For the sloshing model we propose a method to combine liquid sloshing with the general free-floating robot dynamics.

To accomplish this task we assume that the manipulator is equipped with joint position and torque sensors and the standard GNC (Guidance Navigation and Control) sensors on board. Finally, numerical simulations are done do show the feasability of the proposed method.

B. Related Work

The authors in [3] use an on-line parameter adaptation for a handled load and a flexible manipulator arm by minimizing the end effector positions. An alternative method to estimate vibrations of flexible space structures is presented in [4] by the use of range imaging sensors. In [5] a flexible space manipulator is modeled with the help of finite element methods and an adaptive control is proposed with actively damping out the flexible motions of the arm during maneuvering.

For modelling and identifying fuel sloshing there are several methods proposed in the literature. In general they use two main approaches for mechanical equivalent models: multi mass spring-damper equivalent and the pendulum equivalent. The authors in [1], [6], [7] use the pendulum equivalent modelling for lateral sloshing analysis. For the sloshing fuel mass a pendulum mass is used. To define the equivalent pendulum length, pendulum mass, spring and damping constants, they carried out one-DoF (degree of freedom) lateral experiments with different fuel types with a sensor equipped simplified fuel tank. The parameters are identified with a MATLAB Parameter Estimation Toolbox. One result they propose is, that the fuel viscosity and hence the type of fuel has no effect to the pendulum length and the slosh frequency. To model more than one modes multi pendula models are used, e.g. in [8] and [9]. Multi mass spring models are alternatively used in [10]–[12].

To obtain the right parameters for the pendulum equivalent of a defined tank and fuel configuration, there are some one-DoF experiments described in the literature, which use simple lateral acceleration profiles to identify the unknown parameters (e.g. [1] and [13]). But these methods need to know the fill level of the tank and must be carried out on

The authors are with the German Aerospace Center (DLR), Institute of Robotics and Mechatronics, D-82234 Wessling, Oberpfaffenhofen, Germany
Contact: wolfgang.rackl@dlr.de

ground with extra measurement equipment like force-torque sensors.

II. Method Description

In this paper we focus on two disturbing dynamic effects, which the free-floating robot control has to cope with during a realistic OOS mission: flexible appendages and liquid fuel sloshing. In Fig. 1 the principle parts of the focused OOS system is sketched. The manipulator is assumed to have both rigid joints and link.

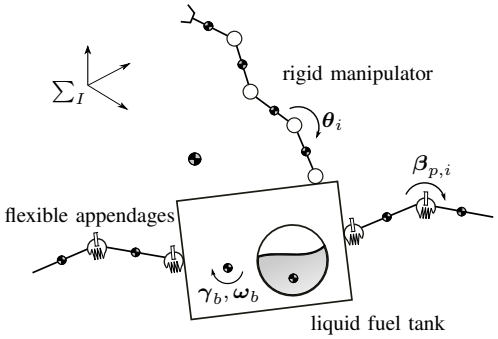

Fig. 1: Principle free-floating robot with flexible appendages and liquid fuel tank with manipulator joint position θ_i, flexible joint position $\beta_{p,i}$, γ_b and ω_b as orientation and angular velocity of the base satellite respectively

In this paper, we analyze both effects separately to see their influence to the parameter identification process.

A. Flexible Appendages

1) Model Description: For modelling flexible appendages like solar panels we assume rigid panel plates and flexible rotational joints connecting the panel plates. The general equation of motion for free-flying robots without any external forces and moments is extended with solar panels connected with rotational joints. The robotic manipulator itself is assumed to have no flexible joints. For a free floating system with n manipulator links and m flexible panel segments the equation of motion can be expressed as

$$\mathbf{H}\ddot{\boldsymbol{y}} + \mathbf{C} + \mathbf{K}\delta\boldsymbol{y} + \mathbf{D}\dot{\boldsymbol{y}} = \boldsymbol{\tau} \tag{1}$$

with

$$\mathbf{H} = \begin{bmatrix} \mathbf{H}_b & \mathbf{H}_{bm} & \mathbf{H}_{bp} \\ \mathbf{H}_{bm}^T & \mathbf{H}_m & \mathbf{H}_{mp} \\ \mathbf{H}_{bp}^T & \mathbf{H}_{mp}^T & \mathbf{H}_p \end{bmatrix} \tag{2}$$

$$\ddot{\boldsymbol{y}} = \begin{bmatrix} \ddot{\boldsymbol{x}}_b \\ \ddot{\boldsymbol{\theta}}_m \\ \ddot{\boldsymbol{\beta}}_p \end{bmatrix} \quad , \mathbf{C} = \begin{bmatrix} \mathbf{c}_b \\ \mathbf{c}_m \\ \mathbf{c}_p \end{bmatrix} \tag{3}$$

$$\mathbf{K} = \begin{bmatrix} \mathbf{0} \\ \mathbf{0} \\ -diag(k_{i,p}) \end{bmatrix} \quad , \mathbf{D} = \begin{bmatrix} \mathbf{0} \\ \mathbf{0} \\ -diag(d_{i,p}) \end{bmatrix} \tag{4}$$

and

$$\delta\boldsymbol{y} = \begin{bmatrix} \mathbf{0} \\ \mathbf{0} \\ (\boldsymbol{\beta}_p - \boldsymbol{\beta}_{p,0}) \end{bmatrix} \quad , \boldsymbol{\tau} = \begin{bmatrix} \mathbf{0} \\ \boldsymbol{\tau}_m \\ \mathbf{0} \end{bmatrix} \tag{5}$$

where $\mathbf{H}_b \in \mathbb{R}^{6\times6}$, $\mathbf{H}_m \in \mathbb{R}^{n\times n}$, $\mathbf{H}_{bm} \in \mathbb{R}^{6\times n}$, $\mathbf{H}_{bp} \in \mathbb{R}^{6\times m}$, $\mathbf{H}_{mp} \in \mathbb{R}^{n\times m}$ and $\mathbf{H}_p \in \mathbb{R}^{m\times m}$ are the inertia matrices of the satellite base (index b), manipulator (index m), panel (index p) and coupling inertia matrix between the base, the manipulator and the panel segments, respectively. The vectors $\mathbf{c}_b \in \mathbb{R}^{6\times1}$ and $\mathbf{c}_m \in \mathbb{R}^{n\times1}$ and $\mathbf{c}_p \in \mathbb{R}^{m\times1}$ are the non-linear velocity dependent term on the base, on the manipulator and the panel segments, respectively. The term $\boldsymbol{\tau}_m \in \mathbb{R}^{n\times1}$ depicts the internal joint torques of the manipulator.

The diagonal matrix $\boldsymbol{K} \in \mathbb{R}^{m\times m}$ contains the stiffness parameters k_i of each flexible panel joint and the diagonal matrix $\boldsymbol{D} \in \mathbb{R}^{m\times m}$ contains the velocity depending viscous damping parameters d_i.

The generalized coordinates for the base $\mathbf{x}_b \in \mathbb{R}^{6\times1}$ is composed of the position and orientation (Euler angles) vector $\mathbf{x}_b = [\mathbf{r}_b, \boldsymbol{\gamma}_b]^T$, $\boldsymbol{\theta}_m \in \mathbb{R}^{n\times1}$ depicts the manipulator joint positions and the vector $\boldsymbol{\beta}_p \in \mathbb{R}^{m\times1}$ describes the panel joint deflection. The variables $\mathbf{x}_b$ (since we are assuming a free floating robot) and $\boldsymbol{\beta}_p$ are assumed to be not actuated and $\boldsymbol{\beta}_{p,0}$ is the initial panel deflection and is defined here for all panel joints to

$$\boldsymbol{\beta}_{p,0,i} = 0 \tag{6}$$

2) Excitation: For the identification of the flexible modes of the flexible appendages we use manipulator maneuvers to excite the modes and we assume an a priori knowledge of the orientation of their rotational axis. For reasons of simplification we assume all flexible joints to be parallel. To obtain the highest impact with the highest system answer we propose to obtain in general with a satellite angular base acceleration parallel to the flexible joint acceleration as

$$\dot{\boldsymbol{\omega}}_b \parallel \dot{\boldsymbol{\beta}}_{p,i} \tag{7}$$

The satellite translational acceleration should be both parallel to the translational motion of the CoM of the flexible appendage and perpendicular to the flexible joint connection vector, e.g. solar panel surface:

$$\ddot{\boldsymbol{r}}_b \perp \ddot{\boldsymbol{r}}_{p,i} \vee \ddot{\boldsymbol{r}}_b \perp \boldsymbol{r}_{p,i\to p,i+1} \tag{8}$$

Since we are dealing with a not actuated satellite base we have to generate such motion vector with the manipulator.

Trajectory Optimization: To obtain a trajectory fulfilling the conditions for well-excited flexible modes, we use a B-spline parametrization, as we proposed in [14]. The trajectory optimization is addressed here as a nonlinear optimization problem with constraints. The optimization problem contains a configuration space C of dimensions $C(\boldsymbol{\theta}) \subseteq \Re^n$, where n is the number of robot joints to be optimized and $\boldsymbol{\theta}$ is the vector of joint positions . The time interval for the spline is t_f. The optimization problem can be formulated as

$$\min_{\theta, t_f} \Gamma \tag{9}$$

where Γ as cost function and defined as the sum of the scalars of the components of the base angular acceleration parallel to the flexible joints:

$$\Gamma = \left(\sum_{j=0}^{h} \dot{\omega}_{b,j \| \beta_p} \right)^{-1} \tag{10}$$

where the summand is the reciprocal of the sum of the mentioned component of the angular base acceleration over a certain number of preselected points h along the trajectory.

As a simplified approach, as many manipulator joints as possible can be configured to be parallel to the flexible joints and only these joints move with the allowed maximum speed and acceleration (close to dirac impulse).

3) Identification: For the free-floating robot system we assume to be known the manipulator parameter. The parameters to be estimated are defined for the described system as

- natural frequency ω_n
- mass, center of mass and inertia matrix of the satellite base and the flexible appendages
- stiffness matrix $\mathbf{K}_p$
- damping matrix $\mathbf{D}_p$

As first step, we identify the natural frequency with the use of the measured joint torque sensor signals as well as the satellite base angular velocity signals (gyros). Note, the joint torque sensor is assumed to be after the joint gear to measure only the acting torque without joint friction effects. Applying a Fast Fourier Transformation (FFT) to this signals measured as answer after the excitation, the natural frequency can be obtained.

The remaining parameter are identified with a nonlinear optimization which is defined with the cost function Γ as the sum of all differences between the expected and the measured torques as

$$\Gamma = \sum_{i=1}^{n} \sum_{j=1}^{N} \tau_{i,j} - \tau_{i,j,msr} \tag{11}$$

B. Sloshing

1) Model Description: Computational Fluid Dynamic (CFD) models nowadays come very close to the real behavior of a liquid, but they need very high computational power and time and are not usable for real-time control design. So the most used method to design liquid sloshing for spacecraft control is the equivalent mechanical model. It describes the macroscopic mechanical characteristics very well. There are two different equivalent mechanical models used in the literature: spring-mass equivalent model and pendulum equivalent model. In this work, we used the pendulum analogy. In Fig. 2 the principle of the used fuel sloshing model is shown.

The model consists of two parts: one fixed mass and one or more slosh masses connected to pendulum, spring and damper elements. The fixed mass m_0 is assumed to be non-sloshing and stationary with respect to the tank and affects the total mass and inertia of the satellite. The second

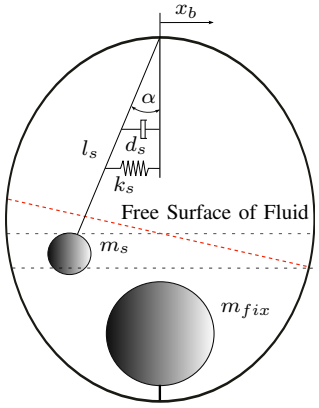

Fig. 2: Dynamic model of fuel sloshing - pendulum equivalent

part represents the moving sloshing part of the fluid m_s. The spring and damper elements take into account effects caused by viscous and friction forces with the tank walls and furthermore forces caused by diaphragm used in pressurized fuel tanks. The pendulum arm is assumed to be massless. The fulcrum of the pendulum is free to rotate in three dimensions like a spherical joint. In this simplified model it is assumed that the sloshing is only a surface wave. In Fig. 2 a free surface is sketched without any diaphragm. The initial pendulum deflection α is assumed to be zero without external disturbance. One pendulum hereby represents one sloshing mode. In our case we want to consider only the first fundamental sloshing mode which is assumed to be dominant in this case.

The equation of motion of the pendulum can be easily set up and should not be repeated here. For reasons of impact to the general free-floating robot dynamics and to the identification process, the generated forces due to the fuel sloshing effect are focused next.

To analyze forces caused by the fuel sloshing acting to the satellite base body during manipulator maneuver, we extract the free body diagram of the sloshing mass in Fig. 3. The

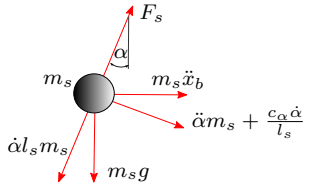

Fig. 3: Free body diagram for the slosh mass

forces acting on the tank can be split up into a force due to the acceleration of the mass, centripetal force, gravity force and damping force. The sum related to the body diagram can be written as

$$\sum \mathbf{F}_{s,lat} = m_s \ddot{\mathbf{x}}_{b,lat} - \dot{\alpha}^2 l_s m_s sin(\alpha) + \cdots$$
$$\cdots + \left(\ddot{\alpha} l_s m_s + \frac{c_\alpha \dot{\alpha}}{l_s} \right) cos(\alpha) + F_s sin(\alpha) \tag{12}$$

$$\sum \mathbf{F}_{s,axial} = m_s \ddot{\mathbf{x}}_{b,axial} - \dot{\alpha}^2 l_s m_s cos(\alpha) + \cdots$$
$$\cdots + \left(\ddot{\alpha} l_s m_s + \frac{c_\alpha \dot{\alpha}}{l_s} \right) sin(\alpha) + F_s cos(\alpha) \quad (13)$$

Note, a rotational viscous damper with the coefficient c_α is included in the damping term in the equations above. To analyze the contribution of certain force parts described above, we assume a small angle approximation and can solve the resulting slosh force to the satellite base as follows:

$$\mathbf{F}_{s,lat} = m_s \ddot{\mathbf{x}}_{b,lat} + \left(\ddot{\alpha} l_s m_s + \frac{c_\alpha \dot{\alpha}}{l_s} \right) \quad (14)$$

$$\mathbf{F}_{s,axial} = m_s \ddot{\mathbf{x}}_{b,axial} \quad (15)$$

The equations above show clearly that for the same components of the external movement $\ddot{\mathbf{x}}_b$ the lateral force and hence the lateral slosh effect is higher that the axial effect.

Due to the fact that we handle a damped oscillation system, which we are exciting during robotic manipulation, the problem of the natural frequency arises. The slosh mass pendulum frequency can be obtained as [1]

$$\omega_n = \sqrt{\frac{\ddot{x}_{b,axial}}{l_s} + \frac{k_s}{m_s l_s^2}} \quad (16)$$

The parameters of the pendulum equivalent like the pendulum length l_s, the fixed fuel mass m_{fix}, equivalent sloshing mass m_s, stiffness k_s and damping d_s depend strongly on the used fuel tank (geometry, wall friction, use of diaphragm, pressure in tank, geometric slosh damping features) and fuel properties (total fuel mass in the tank and fuel viscosity).

To include the dynamic equivalent slosh model into the general equation of motion for free-floating robots, the 3D-pendulum with spring-damper elements can be modeled as an unactuated, passive robot link. The fulcrum of the pendulum is formulated as wrist kinematics: two serial rotational joints without mass and zero relative distance. The degree of freedom around the fulcrums axis is assumed to be locked since the effect of this motion is assumed to be insignificant. The equation can be expressed similar to (1) as

$$\mathbf{H}\ddot{\boldsymbol{y}} + \mathbf{C} + \mathbf{K}\delta\boldsymbol{\alpha} + \mathbf{D}\dot{\boldsymbol{\alpha}} = \boldsymbol{\tau} \quad (17)$$

with

$$\mathbf{H}_b = \hat{\mathbf{H}}_b + \mathbf{H}_{s,fix} \quad (18)$$

where the terms for the panel in (1) are replaced with the terms for the pendulum.

The matrices $\mathbf{H}_{bs} \in \mathbb{R}^{6\times3}$, $\mathbf{H}_{ms} \in \mathbb{R}^{n\times3}$ and $\mathbf{H}_s \in \mathbb{R}^{3\times3}$ are the inertia matrices of the satellite base (index b), manipulator (index m), sloshing mass (index s) and coupling inertia matrix between the base, the manipulator and the sloshing mass, respectively. The fixed fuel mass is added to the rigid satellite base body parameter and will not appear as an extra parameter to be identified. Further following terms are defined for the sloshing model as $\mathbf{c}_s \in \mathbb{R}^{3\times1}$, $\boldsymbol{K} \in \mathbb{R}^{3\times3}$ contains the sloshing spring constant $k_{s,i}$ for all three dimensions and $\boldsymbol{D} \in \mathbb{R}^{3\times3}$ contains the velocity depending sloshing damping constants $d_{s,i}$.

The generalized coordinate $\boldsymbol{\alpha}_s \in \mathbb{R}^{3\times1}$ describes the pendulum fulcrum deflection and is assumed to be not actuated and defined to be a zero vector in initial condition.

2) Excitation: Since the sloshing model can be defined as a parallel link manipulator with a concentrated mass at the top of the link and connected via a flexible spring damper element, the excitation can be optimized similar to case of flexible appendages, see II-A.2

3) Identification: Similar to the identification of flexible appendages we assume the manipulator as known. The parameters for the sloshing model to be estimated are defined here as

- natural frequency ω_n (Hz)
- Mass, center of mass and inertia matrix of the satellite base and the slosh mass m_s (kg)
- Pendulum length l_s (m)
- Pendulum spring constant k_s (Nm/rad)
- Pendulum damping constant d_s (Nm/rad^2)

For the method of identification we chose the same as for the flexible appendages case, see II-A.3.

III. Numerical Simulation

To investigate the performance of the described methods, numerical simulations were conducted both for the flexible model and the liquid sloshing model. For the simulation we used a 7-DoF redundant manipulator mounted on a base satellite with the total manipulator kinematics length of $l_m = 3\ m$. As flexible appendages we defined two solar panels consisting each of two flexible joints, resulting in a total of 4 flexible joints. For the sloshing model, we used one point mass with a 2 DoF joint connected to the fulcrum of the pendulum. The parameters of the model are listed in Tab. I

TABLE I: Simulation model parameter for the flexible and sloshing model. The index b stands for satellite base, m for manipulator, p for flexible appendages and s for sloshing

Parameter	Value	Unit
m_b	600	kg
CoM_b	$[0.9, 0.0, 0.6]$	m
I_b	$diag(150, 150, 150)$	kgm^2
l_m (total)	3.0	m
m_m (total)	60.0	kg
$I_{m,i},\ \forall i = 1...7$	$diag(0.4, 0.04, 0.4)$	m
$m_{p,i}\ \forall i = 1...4$	33.0	kg
$I_{p,i}\ \forall i = 1...4$	$diag(15.0, 11.0, 15.0)$	kgm^2
$k_{p,i}\ \forall i = 1...4$	200.0	Nm/rad
$d_{p,i},\ \forall i = 1...4$	2.0	Nms/rad
m_s	100.0	kg
l_s	0.8	m
$k_{s,i}\ \forall i = 1...2$	20.0	Nm/rad
$d_{s,i}\ \forall i = 1...2$	5.0	Nms/rad

A. Flexible Appendages

We want to investigate here the influence of flexible appendages on the accuracy of a system identification (mass, center of mass and inertia of the satellite base) in orbit. To achieve this, a simulation with a rigid body free-floating robot was conducted first. With the resulting simulated sensor data (joint positions, joint torques and base angular velocity, here without simulated noise), a rigid body identification was carried out to obtain an identified model. The latter contained the uncertainties of a rigid body identification, resulting from the identification method presented in [2]. This model was used as a refence model for the intended investigation, by generating a reference trajectory about which positioning errors could be computed for successively identified models.

At first, the excitation trajectory was executed with the full flexible model and a rigid body identification was repeated. To quantify the accuracy of the rigid body parameter identification with the flexible model, the difference to the reference trajectory (end effector position and orientation) was computed. The results are listed in Table II (column *Rigid ID*). Both the mean and the maximum difference along this trajectory are given.

In a second step, with the same simulated sensor data of the flexible model a parameter identification including the flexible parameter was carried out. The simulation of the reference trajectory with the resulting identified flexible model was then also compared with the reference simulation. The end effector error of this comparison is shown in the third column of Table II. It can be seen that the flexible appendages on a satellite have measurable significant influence on the rigid body identification, as shown in the *Rigid ID* column, and the parameter identification can be improved with an extension to the flexible model parameters (column *Flex. ID*).

TABLE II: Error of end effector for the flexible model

Error [m,rad]	Rigid ID	Flex. ID
mean pos_E [m]	0.0181	0.0094
max pos_E [m]	0.0210	0.0192
mean rpy_E [rad]	0.1542	0.0584
max rpy_E [rad]	0.2032	0.0921

In Fig. 4 the free motion after the commanded manipulator trajectory is plotted. The oscillating flexible appendages cause a base motion (bottom) which results in measurable robot joint torques (top). In this example, joint 2 and 4 are parallel to the flexible joint axis and show the highest torque signals.

The natural frequency ω_n was estimated out of the joint torque and base velocity data with the Fast Fourier Transformation data of the signals. The generated Power Spectral Density (PSD) of the signals are plotted in Fig. 5.

The first two natural frequencies of the flexible free-floating robot system can be seen in the two peaks of the data plot A) and can be quantified with $\omega_{n,1} = 0.23Hz$ and $\omega_{n,2} = 0.68Hz$. The PSD of the trajectory for the rigid body identification B) shows that it avoids the natural frequencies of the flexible model.

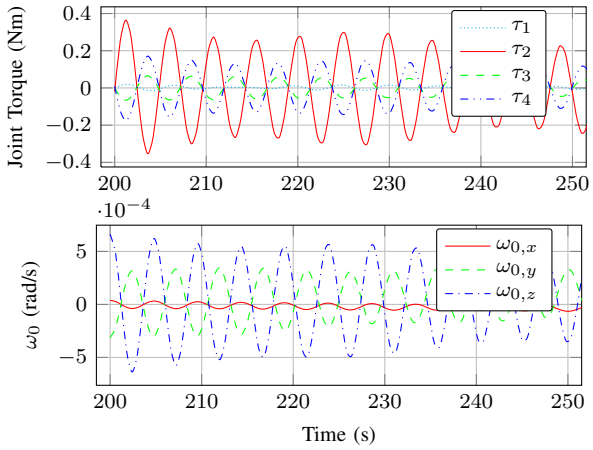

Fig. 4: Answer of the flexible model after excitation (sector). Robot joint torques (top) and angular velocity of the satellite base (bottom)

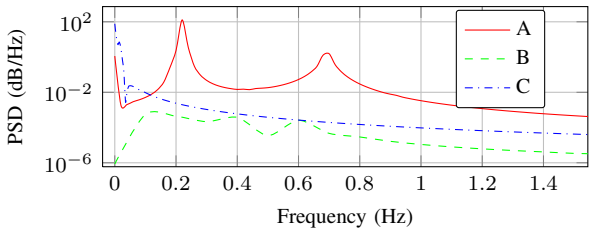

Fig. 5: Power Spectral Density (PSD) of A) answer of the flexible appendages, B) excitation trajectory for flexible modes, C) excitation trajectory for rigid body identification

B. Sloshing

In order to analyze the behavior of the sloshing model in relation to the parameter identification accuracy, we processed similar to that of the flexible model case. Thus, a simulation with an excitation trajectory to excite the sloshing modes was conducted. From the model answer after the excitation the natural frequency was obtained from the simulated sensor data (joint torques and base angular velocity). In Fig. 6 the model answer of the sloshing is plotted. The strong damping of the liquid sloshing can be seen clearly in the significant decrease of the sensor signals. The analysis of the signals transformed into the PSD (A) results in a natural frequency of the sloshing model of $\omega_n = 0.06Hz$ (see Fig. 7). The excitation trajectory for the rigid body identification shows to have the main frequencies below this critical natural frequency (B). The influence of the sloshing parts to the rigid body identification are documented in Table III in the column *Rigid ID*. The data in column *Slosh. ID* prove the improvement of the use of a sloshing identification model.

TABLE III: Error of end effector for sloshing model

Error [m,rad]	Rigid ID	Slosh. ID
mean pos_E [m]	0.0367	0.0214
max pos_E [m]	0.1242	0.0924
mean rpy_E [rad]	0.2319	0.1154
max rpy_E [rad]	0.4291	0.3299

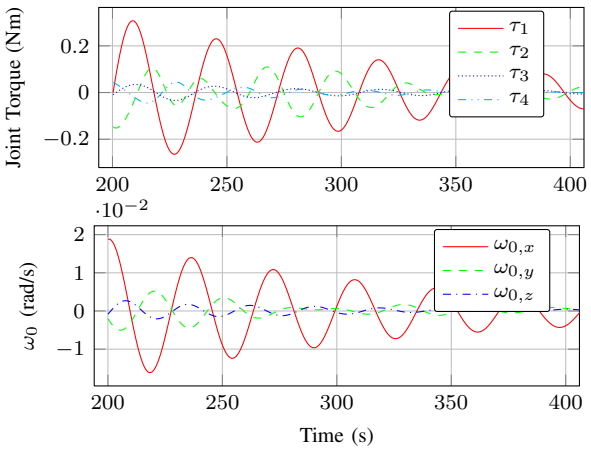

Fig. 6: Answer of the sloshing model after excitation (sector): Joint torques (top) and angular velocity of the satellite base (bottom)

IV. Discussion and Conclusion

The results in the previous section show that flexible appendages mounted on a free-floating satellite can have significant influence to the general dynamics of free-floating robots. For the parameter identification these disturbance effects can be seen clearly. The challenge to excite flexible modes only with the help of the manipulator are the limited constraints of the joint motions in terms of joint velocity and acceleration. Thus, high frequencies can not be excited sufficient. But due to the fact that the expected manipulator motions during an OOS mission will be in a lower frequency range, the analysis in the range below $f = 1.5Hz$ seems to be sufficient.

Liquid sloshing effects are expected to be more critical during an OOS mission due to the fact that the natural frequencies are closer to the expected task motions.

In this paper we focused on the analysis of the general influence of flexible appendages and liquid sloshing to the free-floating dynamics and rigid body parameter identification. For this purpose we extended the parameter identification to both flexible and sloshing effects. The results show in both cases a significant influence to the dynamics and an improvement of the identified dynamic models.

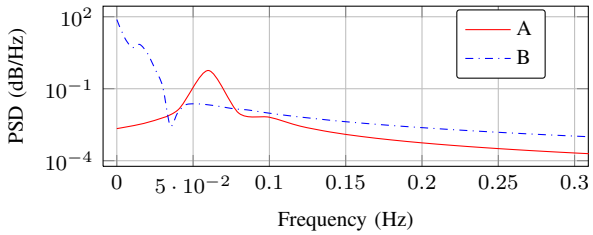

Fig. 7: Power Spectral Density (PSD) of the answer of the sloshing model (A) and the excitation trajectory for rigid body identification (B)

References

[1] Y. Chatman, S. Gangadharan, B. Marsell, and C. Hubert, "Mechanical Analog Approach to Parameter Estimation of Lateral Spacecraft Fuel Slosh," in *49th AIAA/ASME/ASCE/AHS/ASC Structures, Structural Dynamics, and Materials Conference, 16th AIAA/ASME/AHS Adaptive Structures Conference*, ser. , Apr 2008.

[2] W. Rackl, R. Lampariello, and A. Albu-Schäffer, "Parameter identification methods for free-floating space robots with direct torque sensing," in *19th IFAC Symposium on Automatic Control in Aerospace, Wurzburg, Germany*, September 2013.

[3] S. Abiko and K. Yoshida, "On-line parameter identification of a payload handled by flexible based manipulator," in *Intelligent Robots and Systems, 2004. (IROS 2004). Proceedings. 2004 IEEE/RSJ International Conference on*, vol. 3, sept.-2 oct. 2004, pp. 2930 – 2935 vol.3.

[4] M. D. Lichter, H. Ueno, and S. Dubowsky, "Vibration estimation of flexible space structures using range imaging sensors," *The International Journal of Robotics Research*, vol. 25, no. 10, pp. 1001–1012, 2006.

[5] M. Sabatini, P. Gasbarri, R. Monti, and G. B. Palmerini, "Vibration control of a flexible space manipulator during on orbit operations," *Acta Astronautica*, vol. 73, no. 0, pp. 109 – 121, 2012.

[6] K. Schlee, S. Gangadharan, J. Ristow, C. Hubert, J. Sudermann, and C. Walker, "Modeling and parameter estimation of spacecraft fuel slosh mode," in *Simulation Conference, 2005 Proceedings of the Winter*, 2005, p. 10 pp.

[7] K. Schlee, S. Gangadharan, J. Ristow, J. Sudermann, C. Walker, and C. Hubert, "Advanced Method to Estimate Fuel Slosh Simulation Parameters," in *41st AIAA/ASME/SAE/ASEE Joint Propulsion Conference & Exhibit*, ser. Joint Propulsion Conferences. American Institute of Aeronautics and Astronautics, Jul 2005.

[8] M. Reyhanoglu and J. Hervas, "Nonlinear control of a spacecraft with multiple fuel slosh modes," in *Decision and Control and European Control Conference (CDC-ECC), 2011 50th IEEE Conference on*, 2011, pp. 6192–6197.

[9] ——, "Nonlinear control of space vehicles with multi-mass fuel slosh dynamics," in *Recent Advances in Space Technologies (RAST), 2011 5th International Conference on*, 2011, pp. 247–252.

[10] K. Dong, N. Qi, J. Guo, and Y. Li, "An estimation approach for propellant sloshing effect on spacecraft gnc," in *Systems and Control in Aerospace and Astronautics, 2008. ISSCAA 2008. 2nd International Symposium on*, 2008, pp. 1–6.

[11] M. Lazzarin, A. Bettella, M. Manente, and R. D. Forno, "Analytical Sloshing Model and CFD Analysis for the Exomars Mission," in *49th AIAA/ASME/SAE/ASEE Joint Propulsion Conference*, ser. Joint Propulsion Conferences. American Institute of Aeronautics and Astronautics, Jul 2013.

[12] J. Hervas and M. Reyhanoglu, "Control of a spacecraft with time-varying propellant slosh parameters," in *Control, Automation and Systems (ICCAS), 2012 12th International Conference on*, 2012, pp. 1621–1626.

[13] K. Schlee, S. Gangadharan, J. Ristow, J. Sudermann, C. Walker, and C. Hubert, "Modeling and Parameter Estimation of Spacecraft Fuel Slosh Using Pendulum Analogs," in *AIAA/ASME/ASCE/AHS/ASC 47th Structures, Structural Dynamics and Materials (SDM) Conference, New Port, Rhode Island*. American Astronautical Society, May 1-4 2006.

[14] W. Rackl, R. Lampariello, and G. Hirzinger, "Robot excitation trajectories for dynamic parameter estimation using optimized b-splines," in *Robotics and Automation (ICRA), 2012 IEEE International Conference on, St. Paul, Minnesota, USA*, May 2012, pp. 2042 –2047.